Human Molecular Genetics, 2000, Vol. 9, No. 14 **2107–2116**

ARTICLE

Mutations in the *CNGB3* gene encoding the β-subunit of the cone photoreceptor cGMP-gated channel are responsible for achromatopsia (*ACHM3*) linked to chromosome 8q21

Susanne Kohl[1], Britta Baumann[1], Martina Broghammer[1], Herbert Jägle[2], Paul Sieving[3], Ulrich Kellner[4], Robert Spegal[5], Mario Anastasi[6], Eberhart Zrenner[1], Lindsay T. Sharpe[2] and Bernd Wissinger[1+]

[1]Molekulargenetisches Labor and [2]Psychophysisches Labor, Universitäts-Augenklinik, Auf der Morgenstelle 15, D-72076 Tübingen, Germany, [3]Kellogg Eye Center, University of Michigan, Ann Arbor, MI, USA, [4]Augen-Poliklinik, Universitätsklinikum Benjamin Franklin, Berlin-Steglitz, Germany, [5]Micronesia Human Resource Development Center, Kolonia, Pohnpei State, Federated States of Micronesia and [6]Clinica Oculistica, Palermo, Italy

Received 26 May 2000; Revised and Accepted 28 June 2000 DDBJ/EMBL/GenBank accession no. AF272900

Achromatopsia is an autosomal recessive disorder featuring total colour blindness, photophobia, reduced visual acuity and nystagmus. While mutations in the *CNGA3* gene on chromosome 2q11 are responsible for achromatopsia in a subset of patients, previous linkage studies have localized another achromatopsia locus, *ACHM3*, on chromosome 8q21. Using achromatopsia families in which *CNGA3* mutations have been excluded, we refined the *ACHM3* locus to a 3.7 cM region enclosed by markers *D8S1838* and *D8S273*. Two yeast artificial chromosome (YAC) contigs covering nearly the entire *ACHM3* interval were constructed. Database searches with YAC content sequences identified two overlapping high throughput genomic sequencing phase (HTGS) entries which contained sequences homologous to the murine *cng6* gene encoding the putative β-subunit of the cone photoreceptor cGMP-gated channel. Using RT–PCR and RACE, we identified and cloned the human cDNA homologue, designated *CNGB3*, which encodes an 809 amino acid polypeptide. Northern blot analysis revealed a major transcript of ~4.4 kb specifically expressed in the retina. The human *CNGB3* gene consists of 18 exons distributed over ~200 kb of genomic sequence. Analysis of the *CNGB3* gene in achromats revealed six different mutations including a missense mutation (S435F), two stop codon mutations (R203X and E336X), a 1 bp and an 8 bp deletion (1148delC and 819–826del) and a putative splice site mutation of intron 13. The 1148delC mutation was identified recurrently in several families, and in total was present on 11 of 22 disease chromosomes segregating in our families.

INTRODUCTION

Achromatopsia (rod monochromacy, total colour blindness) is a rare, autosomal recessively inherited ocular disorder characterized by low visual acuity, central scotoma, nystagmus, photophobia and the complete disability to discriminate between colours (1). Electroretinographic recordings (ERGs) in patients show that rod photoreceptor function is normal, whereas cone photoreceptor function cannot be established.

Recently, we showed that mutations in the *CNGA3* gene cause achromatopsia linked to the *ACHM2* locus on chromosome 2q11 (2). *CNGA3* encodes the α-subunit of the cGMP-gated channel in cone photoreceptors, a key player of the phototransduction cascade responsible for the membrane hyperpolarization on light stimulation of photoreceptors. Analysis of the homologous knock-out mouse model showed complete absence of physiologically measurable cone function, decrease in the number of cones in the retina and morphological abnormalities of the remaining cones (3).

However, achromatopsia in man is not a genetically homogenous condition. Linkage analysis in pedigrees from the Pingelap islander population and a large Irish pedigree excluded the *ACHM2*/*CNGA3* locus but detected linkage with markers on chromosome 8q21 and defined a new achromatopsia locus *ACHM3* (4,5). Homozygosity intervals identified in the Pingelap pedigrees localized the *ACHM3* locus to an interval of ~5 cM between markers *D8S1757* and *D8S273*. Yet no cone

[+]To whom correspondence should be addressed. Tel: +49 7071 2985032; Fax: +49 7071 295725; Email: wissinger@uni-tuebingen.de

photoreceptor-specific candidate gene has been mapped to this region, making it necessary to employ positional cloning strategies to identify the gene responsible for *ACHM3*.

Here we report the genetic and physical mapping of the *ACHM3* region, the identification and cloning of the *CNGB3* gene within the critical region and the detection of mutations responsible for achromatopsia linked to chromosome 8q21.

RESULTS

Genetic mapping

We defined a subset of 11 achromatopsia families based on the exclusion of *CNGA3* mutations and discordant marker segregation for the corresponding *ACHM2* locus on chromosome 2q11 (Fig. 1A). Linkage analysis in the combined set of families with polymorphic markers spanning an interval of ~20 cM on chromosome 8q21 resulted in a two-point LOD score of >3.0 for markers *D8S1697*, *D8S1838*, *D8S167* and *D8S273*. The highest combined LOD score of 5.1 was obtained for *D8S1838* at $\theta = 0.0$ (data not shown). The order of markers used for genetic fine mapping was based primarily on published genetic data (6,7; http://www.genethon.fr , http://www.marshmed.org/genetics/) and physical mapping data (8; http://www.genome.wi.mit.edu/cgi-bin/contig/phys-map). The order cen–*D8S543*–*D8S279*–*D8S2324*–*D8S541*–*D8S1705*–*D8S1757*–*D8S275*–*D8S525*–*D8S169*–*D8S1838*–*D8S167*–*D8S1707*–*D8S273*–*D8S88*–*D8S270*–*D8S1699*–*D8S1822*–tel was most consistent with already published data and results herein derived from meiotic breakpoint mapping, homozygosity intervals and sequence-tagged site (STS) content mapping data (see below). On haplotype reconstruction, closest meiotic recombinations were observed for *D8S1757* at the centromeric border in an affected subject (II:1) in family CHRO8 and for *D8S88* at the telomeric border in an unaffected sibling (II:3) in family CHRO17 (Fig. 1B). However, due to the small size of the respective families, those data had to be considered preliminary. Additional mapping evidence was obtained with the observation of significant marker homozygosity intervals in patients from four families (CHRO4, CHRO19, CHRO92 and CHRO183). Among these, a patient of the Pingelap islander population (subject II:1 in family CHRO183) showed homozygosity for eight consecutive markers telomeric to *D8S1838* (Fig. 1B). Taking into account the data reported by Winick *et al.* (4), our results suggest the *ACHM3* locus to be localized within a 3.7 cM region between *D8S1838* and *D8S273*.

Physical mapping

Based on the Whitehead framework map and additional screening efforts, we collected yeast artificial chromosome (YAC) clones mapping to 8q21 in order to build a physical map of the *ACHM3* region. Individual YAC colonies were typed for known short tandem repeat (STR) and STS markers retrieved from public databases (8,9; http://www.genome.wi.mit.edu/cgi-bin/contig/phys-map/ and http://www.ncbi.nlm.nih.gov/genemap/) as well as for additional STSs generated from YAC end and Alu-vectorette PCR products. We thus obtained a YAC contig of ~6.5 Mb size between markers *D8S1757* and *D8S167*, and another contig including marker *D8S273* and further distal markers (Fig. 2). Efforts to cover the gap between both contigs with additional YAC clones from either the CEPH or the ICRF YAC library failed. Right end sequences of both CEPH 790_a_07 and CEPH 952_g_02 clones matched to unordered sequences of the chromosome 8 bacterial artificial chromosome (BAC) clone RP11-386D6 (GenBank accession no. AC021132). BLAST analysis showed that AC021132 also contains *D8S1707*, thus extending the YAC contig to this marker. Similarly, the left end sequence of CEPH 765_g_08 gave a hit to high throughput sequencing phase (HTGS) BAC clone RP11-480D11 (GenBank accession no. AC021991) which also contains STS WI-2030 and overlaps with the finished *D8S273*-containing BAC clone CTB-118P5 (GenBank accession no. AC005066). Sequence sampling of YAC content sequences and their use in database searches proved particularly useful to link unmapped HTGS sequences to the *ACHM3* region. For example, sequences encoding the *IMPA* and the *CA1* genes were identified and placed on the physical map (STS IMPA-PM and SHGC-31642 in Fig. 2).

Identification of the human *CNGB3* gene

The HTGS sequence AC021132 identified with YAC end sequences (see above) virtually overlaps with another HTGS sequence (AC013751) derived from BAC RP11-298P6. Analysis of these sequences with the NIX software package provided significant sequence matches with the mouse *cng6* cDNA encoding the putative β-subunit of the cGMP-gated channel in cone photoreceptors (10).

Amplification of a human genomic segment encompassing sequences homologous to the mouse cDNA with samples of the NIGMS monochromosomal hybrid panel resulted in a product only with DNA from the human chromosome 8 cell line NA10156B, and thus provided additional experimental evidence for the location of *cng6*-homologous sequences on human chromosome 8 (data not shown).

Using primers derived from the *cng6*-homologous human genomic sequence, we performed RT–PCR and RACE experiments with human retinal RNA to amplify and clone the orthologous human cDNA, designated *CNGB3*, according to the HUGO nomenclature committee. Two cDNA species differing in length by 250 bp were identified by 3′ rapid amplification of cDNA ends (RACE). Comparison with the genomic sequence indicated that these different cDNAs represent transcripts with alternative polyadenylation sites. The overlapping cDNA sequences revealed a combined cDNA length of 4119 and 4369 bp, respectively, with an open reading frame of 809 codons from the first in-frame ATG, 46 bp of 5′-untranslated region (UTR) and 1896 bp of 3′-UTR sequence for the longer transcript. Three heterozygous polymorphisms were detected at the cDNA level in directly sequenced RT–PCR products: an A→C single nucleotide polymorphism (SNP) at nucleotide position 892 (nucleotide 1 refers to the first nucleotide of the ATG start codon) resulted in a threonine to proline substitution at amino acid position 298 (T298P) in comparison with the genomic BAC sequence, a silent A→G SNP at nucleotide 2214 and an A→G SNP at nucleotide 2264 exchanging glycine for glutamic acid at amino acid position 755 (E755G). Analysis of the expressed sequence tag database (dbEST) identified only few matching human cDNA sequences, mainly from

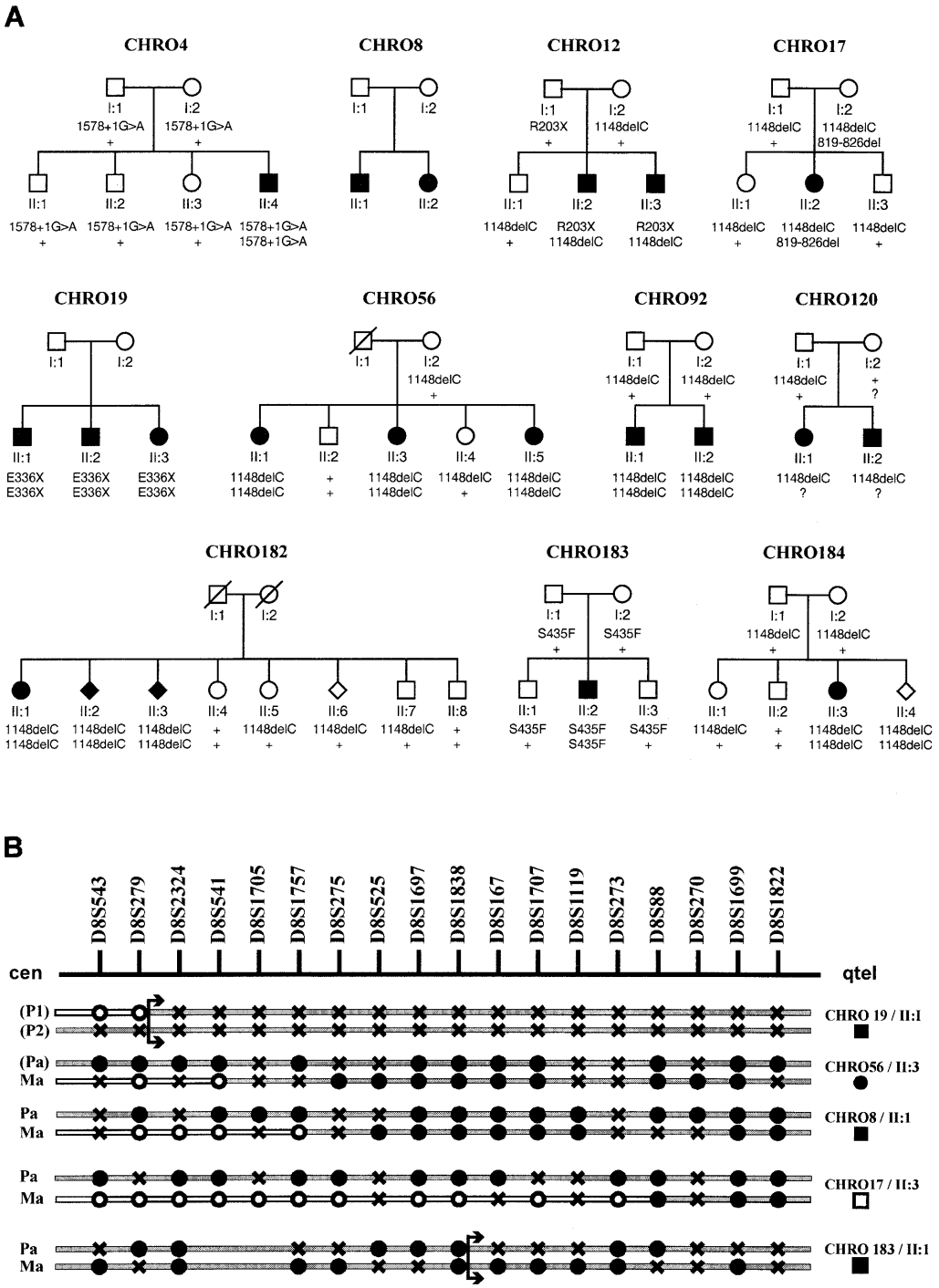

Figure 1. Pedigrees of achromatopsia patients analysed in this study and refined genetic mapping of the *ACHM3* locus. (**A**) Pedigrees of the 11 *ACHM3*-linked achromatopsia families investigated. Segregation of *CNGB3* mutations for available family members is indicated: +, wild-type allele; ?, an as yet unidentified mutation (see text). (**B**) Schematic summary of refined genetic mapping results. Shaded bars represent disease-associated sections, and clear bars recombinant normal sections of chromosome 8q for four affected patients and one unaffected sibling (pedigree identifier and status symbol given on the right) as reconstructed from genotyping of ordered markers from centromere to telomere (top line). The maternal (Ma) and paternal (Pa) origin of the inherited chromosomes is indicated on the left. P1 and P2 indicate unresolved parental origin (both parents not available), and parentheses indicate parental haplotypes reconstructed from the offspring. On the haplotype bars, solid circles represent disease-associated marker alleles, open circles non-disease-associated alleles, and crosses non-informative marker alleles. Sections distal to the arrowheaded brackets represent regions of marker homozygosity in pedigrees CHRO19 and CHRO183.

pineal gland, which cluster in three separate Unigene entries (Hs.114100, Hs.154433 and Hs.180136).

The deduced human CNGB3 polypeptide is 115 amino acids longer than the murine counterpart due to a C-terminal extension. Its molecular mass was calculated as 92.2 kDa and it contains a high proportion of hydrophobic amino acids typical for membrane proteins. Functional domains including transmembrane helices and the cGMP-binding domain are highly

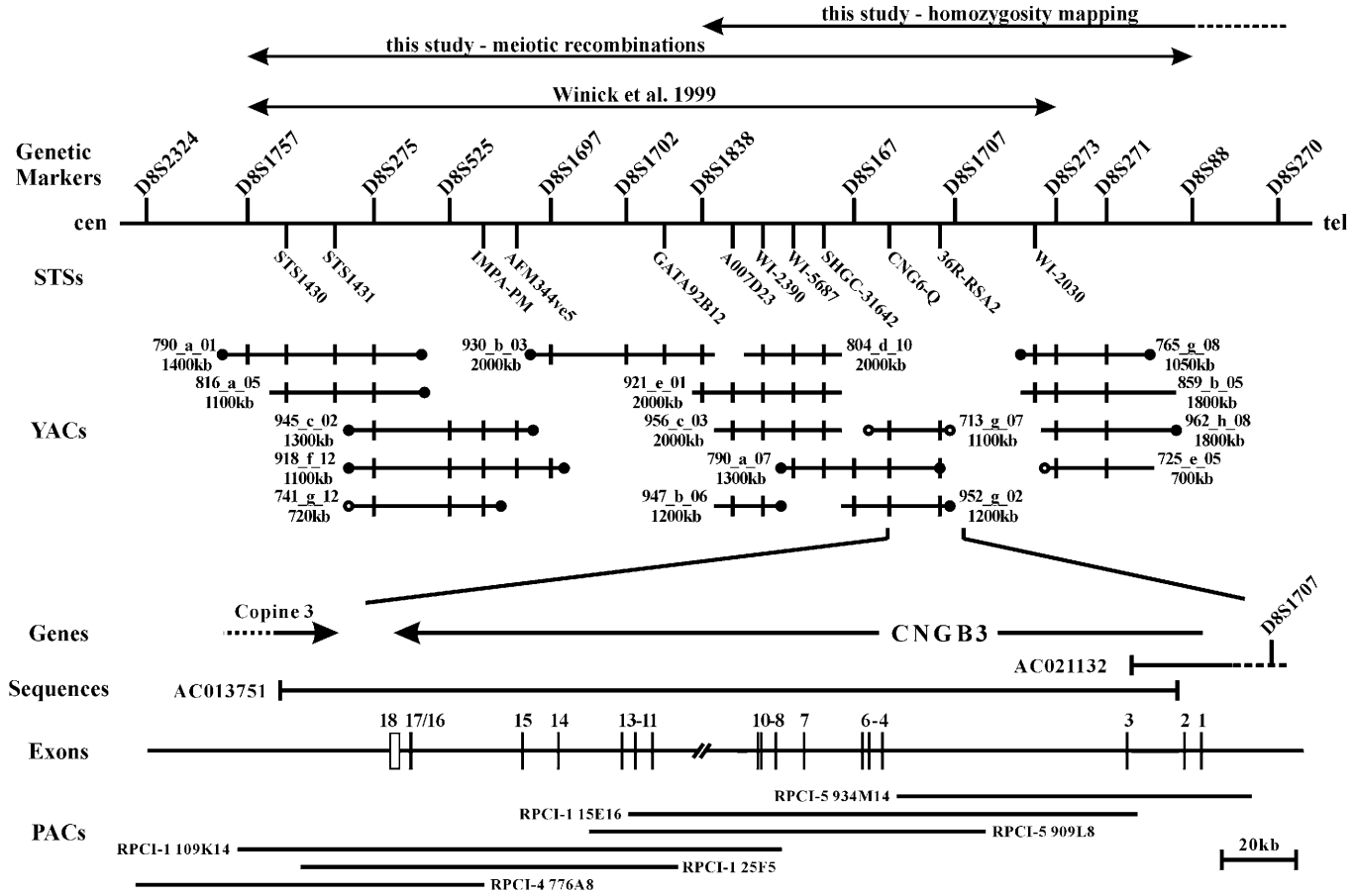

Figure 2. Physical mapping of the *ACHM3* region and location and structure of the *CNGB3* gene. From top to bottom: genetic mapping intervals reported by Winick *et al.* (4) and those found in this study. Below is given the order of genetic markers and STSs used to generate the physical map of the *ACHM3* region. Two non-overlapping YAC contigs were constructed based on STS content mapping. Vertical lines on the individual YAC bars indicate the presence of the respective marker or STS given above. YAC sizes as determined by PFGE are given below the individual YAC address. Filled circles represent YAC end sequences matching various chromosome 8 database sequences by BLAST analysis, and open circles represent end sequences with matches to sequences located on other chromosomes. Below is given an enlarged view of the *CNGB3* region. The *CNGB3* gene is orientated in telomere to centromere direction, and terminal parts of the *Copine 3* gene were found in opposite orientation distal to *CNGB3*. Two HTGS phase sequences AC013751 and AC021132 cover the *CNGB3* region including all exons (1–18) of the *CNGB3* gene. Contigs within the HTGS phase sequences were ordered and experimentally verified by additional PAC clones (bottom).

conserved and display 82% identity at the amino acid sequence level between human and mouse (Fig. 3). Neither the murine *cng6* nor the orthologous human *CNGB3* gene encode sequences similar to the glutamic acid-rich segment (GARP) of the rod cGMP-gated channel β-subunit which is involved in the structural organization of the phototransduction components in rod photoreceptors (11) (Fig. 3).

Northern blot analysis showed a major transcript of ~4.4 kb in human retina (Fig. 4). In addition, much less abundant transcripts of ~3.6 and 3.0 kb were detected after longer exposures. Northern blot and multiple tissue dot-blot hybridizations (data not shown) demonstrated that *CNGB3* transcripts are expressed specifically in the retina. Only after long exposure were some faint signals observed in RNA from testis and the WERI-Rb1 retinoblastoma cell line (data not shown).

Comparison of the cDNA with the genomic sequence (HTGS BAC sequences AC013751 and AC021132) showed that the human *CNGB3* gene is encoded by 18 exons covering ~200 kb of genomic sequence (Fig. 2 and Table 1). Exons 1 and 2 are present on AC021132, whereas the remaining 16 exons are located in AC013751. AC021132 and AC013751 overlap by ~15 kb of non-coding sequence between exons 2 and 3. Links between the unordered sequence pieces in the HTGS entries and the sizes of all but one non-contiguously covered intron sequence were obtained by PCR mapping of individual exons and linking PCR amplification with DNA from additional phage P1-derived artificial chromosomes (PACs) isolated for the *CNGB3* gene (Fig. 2, bottom). The exon sizes of the *CNGB3* gene range between 51 and 2197 bp for the 3′-terminal exon. Exon–intron boundaries show typical sequence features and follow the GT–AG rule, except the splice donor downstream of exon 13 which presents a GC instead of GT (Table 1). In a few instances, the presence of a GC dinucleotide at the 5′ end of an intron has been described (12).

The *CNGB3* gene is orientated in telomere to centromere direction. Downstream of the *CNGB3* gene we could identify eight terminal exons of the *Copine 3* gene also present on AC013751. *CNGB3* and *Copine 3* are arranged in tail-to-tail

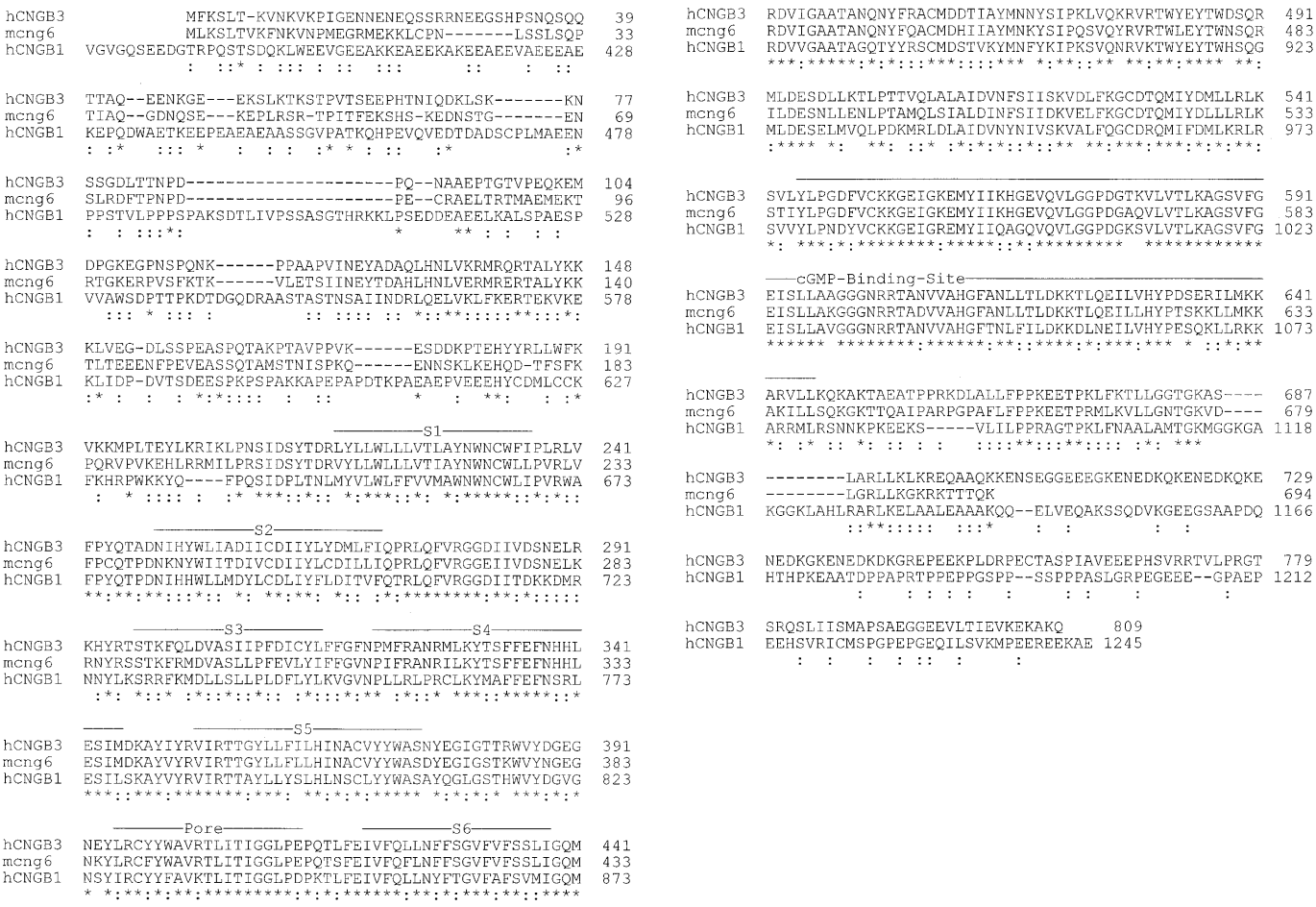

Figure 3. Amino acid sequence alignment of photoreceptor CNG channel β-subunits. Sequence comparison between the human and murine cone photoreceptor β-subunits (hCNGB3, AF272900; mcng6, AJ243572) and the human rod photoreceptor β-subunit (hCNGB1, AF042498). Identical residues in all three sequences are marked by asterisks and residues conserved in two of the three sequences are marked by colons. The position and extent of the six transmembrane helices (S1–S6), the pore and the cyclic nucleotide-binding domain are indicated by lines above the alignment.

configuration and their 3′ ends are separated by ~12.5 kb of genomic sequence (Fig. 2).

Mutations in the *CNGB3* gene in patients with achromatopsia

We then screened the *CNGB3* gene in patients from our 11 *ACHM3*-linked families by direct sequencing of PCR products obtained from amplification of exon segments with primers located in flanking intron or UTR sequences. We identified six different mutations including a missense mutation (1304C→T, S435F), two stop codon mutations (607C→T, R203X and 1006G→T, E336X), two frameshift deletions of 1 and 8 bp (1148delC and 819–826del), respectively, and a putative splice site mutation between exons 13 and 14 (1578+1G→A) (Table 2). Sequence examples of these mutations are outlined in Figure 5. Mutations were found in all *ACHM3*-linked families except CHRO8, and only a single heterozygous mutation was identified in patient II:1 of family CHRO120. Homozygous mutations were present in seven cases, including those in which marker homozygosity intervals were defined initially (Fig. 1). Interestingly, we found the 1 bp deletion mutation (1148delC) recurrently in several patients of different geographic origin. Patients in families CHRO56, CHRO92, CHRO182 and CHRO184 were homozygous for this mutation, and patients in families CHRO12, CHRO17 and CHRO120 harbour this mutation on one of the two disease chromosomes. Patient II:4 in family CHRO4 carried a homozygous G→A substitution at the first nucleotide of intron 13. Thus, the splice donor sequence of this intron is changed from GC to AC. This substitution probably abolishes effective splicing between exons 13 and 14 and thus leads to premature translation termination. Numerous examples of aberrant splicing in cases of G→A substitutions at the first nucleotide position of an intron have been described in the literature (13).

Co-segregation analysis by PCR/restriction fragment length polymorphism (RFLP) or single strand conformation polymorphism (SSCP) was performed in all families and was found to be consistent with the autosomal recessive mode of inheritance in all cases. Moreover, it proved the independent segregation of the mutant alleles (Fig. 6). None of the mutations were found in 100 healthy controls.

The S435F mutation was found to be homozygous in patient II:2 in family CHRO183, originating from the South Pacific

Table 1. Exons and exon–intron boundary sequences of the *CNGB3* gene

Exon	Size (bp)	cDNA sequence[a]	Genomic sequence[b]	Splice acceptor[c]	Splice donor[c,d]
1	175	1–175	132 723–132 549		GCACAGgtatgt
2	82	176–257	128 786–128 705	tgtttttttctcaaagGAAGAA	TACAAGgtcaga
3	127	258–384	131 176–131 302	atttttttttcatagACAAAC	AAACAGgtgagc
4	155	385–539	186 738–186 892	ttttttctcatttagCCCACA	AAACTGgtaagc
5	150	540–689	189 668–189 817	tttttccctatgaagCAAAGC	ACACAGgtatta
6	209	690–898	190 703–190 911	ttgctgtttttccagATCGAC	ATAATAgtaagt
7	51	899–949	203 774–203 824	acaaatatctttcagGTGGAT	TTTCAGgtaggt
8	87	950–1036	12 801–12 715	gtgttctttcaacagTTGGAT	TTAAAGgtaaga
9	65	1037–1101	9600–9536	tgcttttctatatagTACACT	CTACAGgtaaag
10	123	1102–1224	8787–8665	tattctctctgacagAGTTAT	AAACGAgtaagt
11	142	1225–1366	35 475–35 616	cttctgttttcacagGTATCT	GGTCAGgtaagc
12	160	1367–1526	39 290–39 449	tatttgtggttttagATGAGA	TGCTAGgtaagc
13	98	1527–1624	42 289–42 386	tttatctttataaagATGAGT	TTCAAGgcaagt
14	84	1625–1708	56 699–56 782	tttctttttatatagGGTTGT	AAAAAGgtgagt
15	119	1709–1827	64 435–64 553	atatttaaaatgtagGGAGAA	AATCAGgtatct
16	147	1828–1974	89 394–89 540	ttttctctcttacagCCTTCT	AGCCAGgtacaa
17	175	1975–2149	89 783–89 957	ctctcttacccacagAGTGCT	GCTCAGgtaata
18	2197	2150–4346	92 517–94 712	aattgctccttccagAAGAAA	

[a]Sequence positions according to GenBank entry AF272900.
[b]Sequence positions within GenBank entries AC021132 (exons 1 and 2) and AC013751 (remaining exons).
[c]Exon sequences in upper case and intron sequences in lower case letters.
[d]The nucleotide mutated in family CHRO4 is underlined.

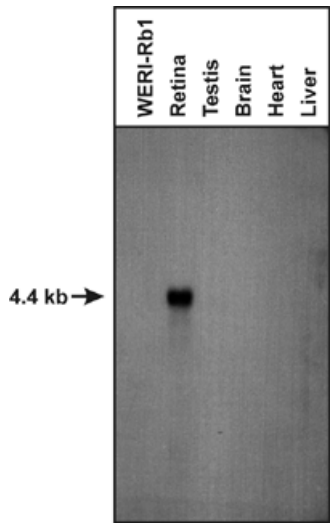

Figure 4. Expression of the human *CNGB3* gene. Northern blot hybridization with a *CNGB3* cDNA probe detected a major transcript of 4.4 kb in retinal RNA. Minor retinal transcripts of ~3.6 and 3.0 kb were detectable after prolonged exposures, as well as low levels of *CNGB3* transcripts in WERI-Rb1 and testis RNA samples (data not shown).

islander population known to exhibit a dramatically increased gene frequency for achromatopsia (14,15). The S435F mutation is located in transmembrane domain S6 and affects an amino acid position conserved between human and mouse and also conserved in the homologous sequence of the rod β-subunit. All other mutations result in a severely truncated polypetide lacking important functional elements, i.e. the pore or the cyclic nucleotide-binding domain, and thus most probably represent null alleles.

Table 2. *CNGB3* mutations in patients with achromatopsia

Location	Alteration in nucleotide sequence[a]	Alteration in polypeptide/mRNA[b]
Exon 5	607C→T	R203X
Exon 6	819–826del	P273fs
Exon 9	1006G→T	E366X
Exon 10	1148delC	T383fs
Exon 11	1304C→T	S435F
Intron 13	1578+1G→A	Splice defect

[a]Sequence position within the *CNGB3* cDNA (GenBank accession no. AF272900) with nucleotide 1 denoting the first nucleotide of the ATG start codon.
[b]fs, frameshift.

DISCUSSION

We have shown recently that mutations in the *CNGA3* gene, which encodes the α-subunit of the cone cGMP-gated channel, are responsible for achromatopsia linked to the *ACHM2* locus on

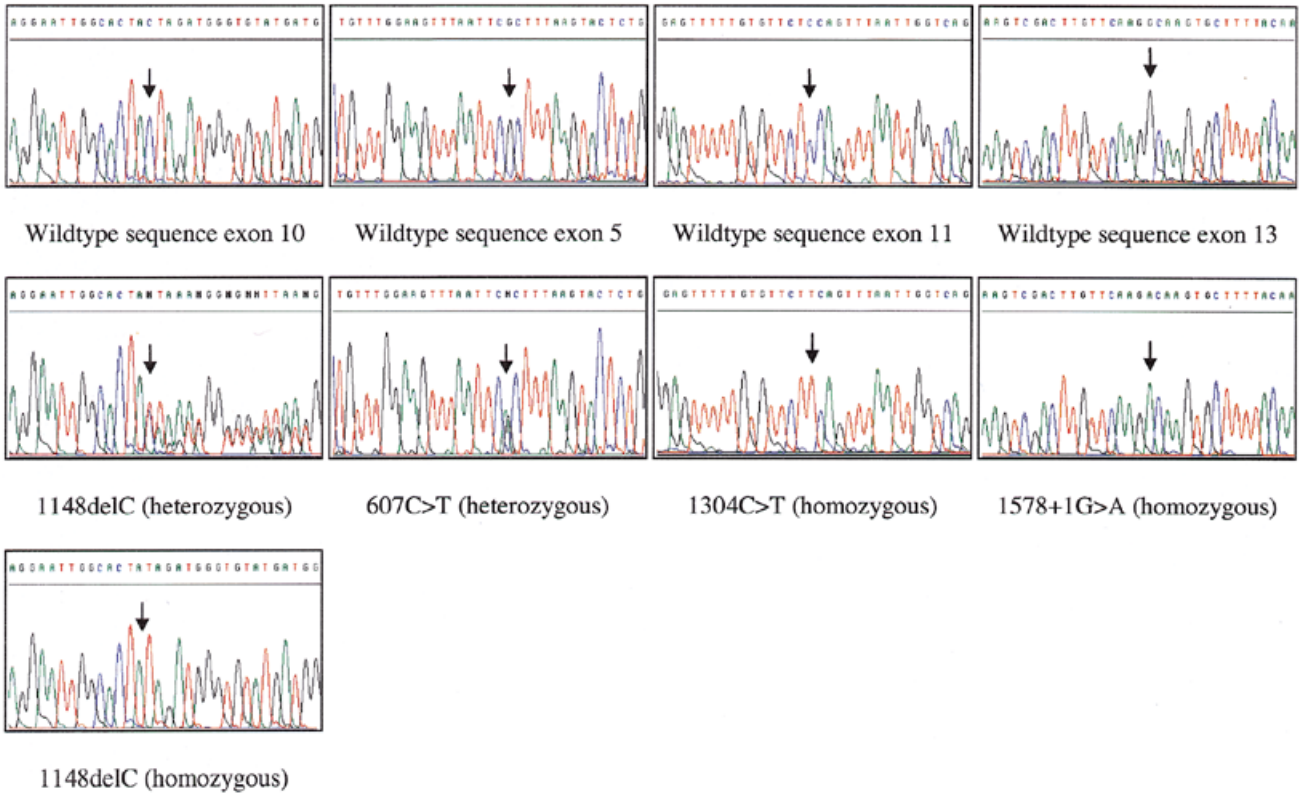

Figure 5. Identification of *CNGB3* mutations in achromatopsia patients. Electropherogram sections of selected heterozygous or homozygous mutant sequences (middle and bottom rows) in comparison with the respective wild-type sequence (top row). The nucleotides altered by the mutations are indicated by arrows.

chromosome 2q11 (2). In this study, we used a positional genomics approach to identify the second gene involved in achromatopsia, *CNGB3*, the gene defective in families linked to the *ACHM3* locus on chromosome 8q21.

Interestingly, *CNGB3* encodes the putative modulatory β-subunit of the cGMP-gated channel of cone photoreceptors. Gerstner *et al.* (10) recently have demonstrated for the mouse orthologue *cng6* that in co-expression experiments the *cng6* gene product modulates the biophysical and electrophysiological behaviour of the functional channel-forming α-subunit. It induces flickering channel gating, a decrease in outward rectification and sensitivity to the blocking agent L-*cis*-diltiazem, similar to native cone cyclic nucleotide-gated (CNG) channels (10).

It has been suggested that native CNG channels represent heterotetramers of two α- and β-subunits (16). In heterologous expression systems, the α-subunit *per se* is able to form functional cation channels (17). In contrast, the β-subunit alone cannot conduct measurable ion currents, although the secondary structure of the polypeptide is conserved between α- and β-subunits, and relevant functional domains (transmembrane helices, pore and cyclic nucleotide-binding domain) are also present in the β-subunit (18). Since mutations in either of the two genes give rise to a clinically indistinguishable phenotype of complete achromatopsia, it has to be assumed that the β-subunit confers some essential function to the native channel complex within the context of phototransduction.

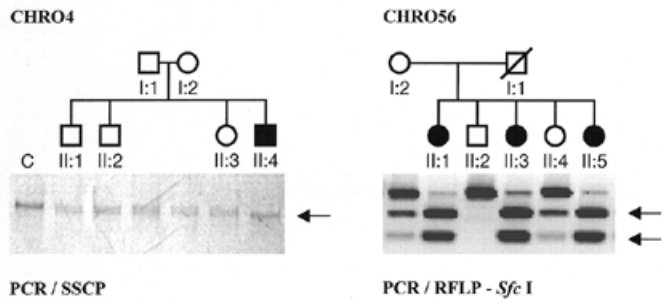

Figure 6. Segregation of *CNGB3* mutations within selected achromatopsia families. Gel lanes are mounted according to the respective subjects in the pedigrees above. The arrows indicate mutant-specific gel bands. (Left) SSCP separation of the 1578+1G→A splice site mutation in family CHRO4. Patient II:4 carries this mutation on both alleles, whereas all siblings and the parents are heterozygous carriers. Lane C, normal control. (Right) Segregation of the 1148delC mutation in family CHRO56 performed by PCR–RFLP analysis with *Sfc*I. All three affecteds are homozygous for this mutation, whereas the mother and sibling II:4 are heterozygous carriers and sibling II:2 does not carry the mutation.

Whereas mutations in the *CNGA3* and *CNGB3* genes cause achromatopsia, a congenital, stationary disorder of the cone photoreceptor system, mutations in the gene for the α-subunit homologue in rod photoreceptors have been shown to cause autosomal recessive retinitis pigmentosa, a progressive form of retinal dystrophy (19). No retinal disorder has yet been

associated with the gene encoding the β-subunit of the rod cGMP-gated channel.

We have identified mutations in the *CNGB3* gene in all but one of our *ACHM3*-linked achromatopsia families. No mutations could be identified in family CHRO8 and only a single heterozygous mutation was detected in family CHRO120. The simplest explanation for this is that these missing mutations are located in an as yet unidentified regulatory region of the *CNGB3* gene, i.e. the promoter region, or that some disease alleles constitute larger deletions unable to be detected by our screening strategy. However, due to the low statistical significance of linkage to the *ACHM3* locus in the individual family, we cannot exclude that achromatopsia in family CHRO8 is not caused by mutations in the *CNGB3* gene but by another gene defect.

The 1 bp deletion mutation, 1148delC, was found recurrently in our patient sample. In total, 11 of the 22 disease chromosomes carry this common mutation. Haplotype analysis based on linked microsatellite markers provided no significant evidence for a linkage disequilibrium among chromosomes carrying the 1148delC mutation (data not shown). Additional studies with a larger number of disease chromosomes and inclusion of closely spaced, robust markers (i.e. SNPs) will be necessary to address the question on the origin of this particular mutation. Another reason for its high frequency might be that this particular nucleotide position is prone to deletion and thus represents a mutational hot spot. Several other examples of disease genes with a high frequency of particular deletion mutations either due to a founder effect or recurrent new mutation have been described, i.e. *CFTR* (20), *GJB2* (21) and *USH2A* (22).

The *ACHM3* locus was mapped originally to chromosome 8q21 in pedigrees from a South Pacific islander population, in which achromatopsia is highly frequent and affects nearly 10% of the native population. Therefore, this conditon has also been acknowledged as Pingelapese blindness (OMIM 262300). It has been assumed that this >1000-fold increased incidence in comparison with the European population (23) results from genetic drift following a devastating typhoon in the 18th century killing most of the inhabitants. These instances have come to public attention through Oliver Sacks' book *The Island of the Colorblind* (14) and a recent BBC television documentary (24). Family CHRO183 investigated in this study originates from this particular population. Since we have identified a homozygous S435F mutation as the sole alteration in the *CNGB3* gene in this family, we argue that this particular mutation is the cause of Pingelapese blindness.

MATERIALS AND METHODS

Achromatopsia patients

Caucasian patients were enrolled at several clinical centres in Germany (Tübingen, Berlin), the USA (Ann Arbor, MI) and Italy (Palermo). The clinical diagnosis of achromatopsia was based on ophthalmological examination including ERG recordings, fundus examination, visual acuity and visual field testing, and standard colour vision analysis. In addition, this study included a family from a South Pacific islander population, in which achromatopsia is highly frequent (14,15).

Blood samples from patients and family members were collected after informed consent. Total genomic DNA was extracted from the blood samples according to standard procedures (25).

Marker analysis

Seventeen polymorphic STR markers spanning a region of ~20 cM on human chromosome 8q21 (6,7) were genotyped by means of PCR amplification with fluorescence-labelled primers and electrophoretic sizing on an ABI 373 DNA sequencer (PE Biosystems, Weiterstadt, Germany) as described previously (26).

Statistical methods and haplotype reconstruction

Two-point LOD scores were calculated using the LINKAGE program package (27). A disease allele frequency of 0.005 and a penetrance of 1.0 were taken for calculations. Marker allele frequencies were assumed to be equal. Haplotypes were reconstructed manually, minimizing the number of recombinations.

Isolation and analysis of YAC clones

Individual YAC clones positive for chromosome 8q21 STSs were obtained from the German Human Genome Resource Center (RZPD, Berlin, Germany) or Research Genetics (Huntsville, AL). In addition, DNA pools of the CEPH Mark I and Mark II YAC libraries were screened by PCR to identify additional clones for known and newly developed STSs. Preparation of total yeast DNA and agarose plugs for pulsed-field gel electrophoresis (PFGE) was performed as previously described (26) or following standard procedures (28). YAC sizes were determined by probing PFGE blots with ^{32}P-labelled human cot-1 DNA to visualize artificial chromosomes.

STS content mapping was done with 5 ng of total yeast DNA and PCRs limited to 25 thermal cycles.

Isolation of YAC sequences and STSs

YAC end sequences were isolated by established vectorette PCR methods (28). In addition, internal YAC sequences were obtained by Alu vectorette PCR: briefly, 200 ng of total yeast DNA was digested separately with *Alu*I, *Rsa*I, *Pvu*II, *Bsp*143I, *Bgl*II or *Bam*HI, and ligated with compatible double-stranded vectorettes. Vectorette libraries were subjected to PCR amplification with vectorette and Alu repeat primers; products were size selected and cloned with the TA Cloning System (Invitrogen, Groningen, The Netherlands). Purified plasmid DNA was then sequenced with standard pUC/M13 forward and reverse primers. The chromosomal origin of newly developed STSs was determined by PCR amplification using selected DNA samples (NA10156B, NA14064 and NA11619) of a chromosome 8 regional mapping panel (Coriell Institute, Camden, NJ).

PAC isolation and analysis

Human PAC clones from the RPCI 1,3-5 library were identified by screening high density clone filters (provided by the RZPD) with ^{32}P-labelled probes. PAC DNA was isolated by standard alkaline lysis methods. Insert sizes were determined by PFGE separation of *Not*I-digested PAC DNA. STS content

mapping was done with 500 pg of PAC DNA and PCRs restricted to 23 thermal cycles.

Northern blot and RNA dot-blot hybridization

A human multiple tissue dot-blot (no. 7775-1) and total RNA from human brain, testis and liver were purchased from Clontech (Heidelberg, Germany). In addition, total RNA was isolated from human donor retinae and the human retinoblastoma cell line WERI-Rb-1 using Trizol reagent (Life Technologies, Eggenstein, Germany). For northern blots, 6 µg of total RNA of each sample were separated on a 1% agarose gel containing 2.2 M formaldehyde and blotted onto a Hybond-N nylon membrane (Amersham Pharmacia, Freiburg, Germany).

A cDNA fragment encompassing nucleotides 1–2323 of the *CNGB3* cDNA was labelled with [α-^{32}P]dCTP using the NEBlot kit (New England Biolabs, Schwalbach, Germany) and used for hybridization in ExpHyb solution (Clontech) for 15 h at 65°C. The filter was washed twice in 1× SSC, 0.15% SDS at 40°C and 0.1× SSC, 0.15% SDS at 65–70°C. Blots were exposed against X-ray films for 24–96 h at –80°C with intensifying screens.

RACE and RT–PCR

A 5 µg aliquot of total human retinal RNA was reverse-transcribed into single-stranded cDNA with AMV reverse transcriptase and random 9mer oligonucleotide primers. Aliquots were used to amplify overlapping cDNA fragments of the human *CNGB3* gene. Primer sequences were derived from segments of the human HTGS sequence AC013751 which showed significant homology to the murine *cnga3* cDNA (10).

For 5′ RACE, 20 ng of Marathon-Ready Human Retinal cDNA (Clontech) were subjected to nested PCR amplifications with adaptor primers and primers derived from internal *CNGB3* cDNA sequences. For 3′ RACE, 1 µg of total human retinal RNA was reverse-transcribed with AMV reverse transcriptase and an oligo(dT) adaptor primer (RNA PCR kit; Takara, Shiga, Japan). First strand cDNA was then used for hemi-nested PCR amplifications with adaptor primers, and primers derived from internal *CNGB3* cDNA sequences. RACE products were purified by gel electrophoresis and sequenced directly.

Chromosomal mapping

The chromosomal localization of the *CNGB3* gene was analysed by PCR amplification of a genomic 298 bp fragment encompassing exon 5 with DNA samples of a monochromosomal hybrid mapping panel (NIGMS mapping panel no. 2; Coriell Institute).

Mutation screening and segregation analysis

Coding exon sequences were amplified from patients' genomic DNA with primers located in flanking intron and UTR sequences. PCR products were purified with Qiaquick columns (Qiagen, Hilden, Germany), sequenced using Big Dye Terminator chemistry (PE Biosystems) and separated on an ABI 377 DNA sequencer. Sequence editing and alignments was performed using the Lasergene Software package (DNASTAR, Madison, WI).

Co-segregation analysis and screening of controls were performed by either sequencing, PCR–RFLP analysis (1148delC, gain of an *Sfc*I site; 1304C→T/S435F, loss of a *Bsr*I site) or PCR–SSCP analysis (607C→T/R203X, 819–826del, 1006G→T/E336X and the 1578+1G→A splice site mutation). For SSCP analysis, 10% polyacrylamide gels (acrylamide:bis-acrylamide 37.5:1) containing 10% glycerol were run with 1× TBE for 20 h at 4°C and visualized by silver staining.

Databases and database analysis

BLAST searches against nr, dbSTS, dbEST, GSS and HTGS segments of GenBank were done at the NCBI server (http://www.ncbi.nlm.nih.gov//). Re-analysis of deposited BAC and PAC sequences was done with the NIX package provided by the UK-HGMP service (Hinxton, UK).

Primer sequences

Primer sequences used for STS mapping, RACE, RT–PCR and amplification of *CNGB3* sequences are available from the authors on request.

NOTE ADDED IN PROOF

After acceptance of this paper, Sundin *et al.* reported the independent identification of the *CNGB3* gene and mutations therein in patients with achromatopsia [Sundin *et al*. (2000) *Nature Genet.*, **25**, 289–293]. Due to their limited cDNA sequence information mutations in the paper by Sundin *et al.* could be assigned only provisionally. The reported mutations Pro160 (8 bp del), Thr270 (1 bp del) and Ser322Phe correspond to the mutations 819–826del (Pro273fs), 1148delC (Thr383fs) and 1304C→T (Ser435Phe), respectively, described in this study (Table 2).

ACKNOWLEDGEMENTS

We thank all patients and family members for participating in this study. In addition, we kindly acknowledge contributions by Bernhard Jurklies, Samuel Jacobson, Günter Rudolph, Sten Andreasson, Thomas Rosenberg, Dorit Lev, Frans Cremers, Birgit Lorenz, Claudio Castellan, Pierre Bitoun, E.C. Sener, S. Tatlipinar and Nurten Akarsu for the collection of achromatopsia families during the course of this research project. Francis Futterman provided much valuable information on achromatopsia and helped with logistic coordinations. We also thank Eva Weber and Sabine Tippmann for excellent technical assistance, and Benjamin Kaupp and Dimitri Tränker for encouraging discussions. We kindly acknowledge the provision of filters and clones by the Resource Center of the German Human Genome Project (RZPD, Berlin) and the availability of bioinformatics services at the UK-HGMP (Hinxton, UK). This work was supported by grants IB2 and Q1 from the Bundesministerium für Bildung und Forschung (01 KS 9602) and the Interdisziplinäres Zentrum für Klinische Forschung (IZKF) Tübingen to L.T.S. and B.W. and a grant from the Deutsche Forschungsgemeinschaft (SFB430/A5) to B.W.

REFERENCES

1. Sharpe, L.T. and Nordby, K. (1990) Total colour blindness: an introduction. In Hess, R.F., Sharpe, L.T. and Nordby, K. (eds), *Night Vision: Basic*, *Clinical and Applied Aspects*. Cambridge University Press, Cambridge, UK.
2. Kohl, S., Marx, T., Giddings, I., Jägle, H., Jacobson, S., Apfelstedt-Sylla, E., Zrenner, E., Sharpe, L.T.S. and Wissinger, B. (1998) Total colour-blindness is caused by mutations in the gene encoding the α-subunit of the cone photoreceptor cGMP gated cation channel. *Nature Genet.*, **19**, 257–259.
3. Biel, M., Seeliger, M., Pfeifer, A., Kohler, K., Gerstner, A., Ludwig, A., Jaissle, G., Fauser, S., Zrenner, E. and Hofmann, F. (1999) Selective loss of cone function in mice lacking the cyclic nucleotide-gated channel CNG3. *Proc. Natl Acad. Sci. USA*, **96**, 7553–7557.
4. Winick, J.D., Blundell, M.L., Galke, B.L., Salam, A.A., Leal., S.M. and Karayiorgou, M. (1999) Homozygosity mapping of the achromatopsia locus in the Pingelapese. *Am. J. Hum. Genet.*, **64**, 1679–1685.
5. Milunsky, A., Huang, X.L., Milunsky, J., DeStefano, A. and Baldwin, C.T. (1999) A locus for autosomal recessive achromatopsia on human chromosome 8q. *Clin. Genet.*, **56**, 82–85.
6. Dib, C., Faure, S., Fizames, C., Samson, D., Drouot, N., Vignal, A., Millasseau, P., Marc, S., Hazan, J., Seboun, E. *et al*. (1996) Comprehensive genetic map of the human genome based on 5,264 microsatellites. *Nature*, **380**, 152–154.
7. Broman, K.W., Murray, J.C., Sheffield, V.C., White, R.L. and Weber, J.L. (1998) Comprehensive human genetic maps: individual and sex-specific variation in recombination. *Am. J. Hum. Genet.*, **63**, 861–689.
8. Hudson, T.J., Stein, L.D., Gerety, S.S., Ma, J., Castle, A.B., Silva, J., Slonim, D.K., Baptista, R., Kruglyak, L., Xu, S.H. *et al*. (1995) An STS-based map of the human genome. *Science*, **270**, 1919–1920.
9. Schuler, G.D., Boguski, M.S., Stewart, E.A., Stein, L.D., Gyapay, G., Rice, K., White, R.E., Rodriguez-Tome, P., Aggarwal, A., Bajorek, E. *et al*. (1996) A gene map of the human genome. *Science*, **274**, 540–546.
10. Gerstner, A., Zong, X., Hofmann, F. and Biel, M. (2000) Molecular cloning and functional characterization of a new modulatory cyclic nucleotide-gated channel subunit from mouse retina. *J. Neurosci.*, **20**, 1324–1332.
11. Körschen, H.G., Beyermann, M., Müller, F., Heck, M., Vantler, M., Koch, K.W., Kellner, R., Wolfrum, U., Bode, C., Hofmann, K.P. and Kaupp, U.B. (1999) Interaction of glutamic-acid-rich proteins with the cGMP signalling pathway in rod photoreceptors. *Nature*, **400**, 761–766.
12. Jackson, I.J. (1991) A reappraisal of non-consensus mRNA splice sites. *Nucleic Acids Res.*, **19**, 3795–3798.
13. Krawczak, M., Reiss, J. and Cooper, D.N. (1992) The mutational spectrum of single base-pair substitutions in mRNA splice junctions of human genes: causes and consequences. *Hum. Genet.*, **90**, 41–54.
14. Sacks, O. (1998) *The Island of the Colorblind*. Vintage Books, Random House, New York, NY.
15. Brody, J.A., Hussels, I., Brink, E. and Torres, J. (1970) Hereditary blindness among Pingelapese people of eastern Caroline Islands. *Lancet*, **1**, 1253–1257.
16. Zagotta, W. and Siegelbaum, S.A. (1996) Structure and function of cyclic nucleotide-gated channels. *Annu. Rev. Neurosci.*, **19**, 235–263.
17. Wissinger, B., Müller, F., Weyand, I., Schuffenhauer, S., Thanos, S., Kaupp, U.B. and Zrenner, E. (1997) Cloning, chromosomal localization and functional expression of the gene encoding the α-subunit of the cGMP-gated channel in human cone photoreceptors. *Eur. J. Neurosci.*, **9**, 2512–2521.
18. Chen, T.Y., Peng, Y.W., Dhallan, R.S., Ahamed, B., Reed, R.R. and Yau, K.W. (1993) A new subunit of the cyclic nucleotide-gated cation channel in retinal rods. *Nature*, **362**, 764–767.
19. Dryja, T.P., Finn, J.T., Peng, Y.W., McGee, T.L., Berson, E.L. and Yau, K.W. (1995) Mutations in the gene encoding the α-subunit of the rod cGMP-gated channel in autosomal recessive retinitis pigmentosa. *Proc. Natl Acad. Sci. USA*, **91**, 10177–10181.
20. Kerem, B.-S., Rommens, J.M., Buchanan, J.A., Markiewicz, D., Cox, T.K., Chakravarti, A., Buchwald, M. and Tsui, L.-C. (1989) Identification of the cystic fibrosis gene: genetic analysis. *Science*, **245**, 1073–1080.
21. Denoyelle, F., Weil, D., Maw, M.A., Wilcox, S.A., Lench, N.J., AllenPowell, D.R., Osborn, A.H., Dahl, H.H.M., Middleton, A., Houseman, M.J. *et al*. (1997) Prelingual deafness: high prevalence of a 30delG mutation in the connexin 26 gene. *Hum. Mol. Genet.*, **6**, 2173–2177.
22. Eudy, J.D., Weston, W.D., Yao, S., Hoover, D.M., Rehm, H.L., Ma-Edmonds, M., Yan, D. *et al*. (1998) Mutation of a gene encoding a protein with extracellular matrix motif in Usher syndrome type IIa. *Science*, **280**, 1753–1757.
23. Judd, D.B. (1943) Facts of color-blindness. *J. Opt. Soc. Am.*, **33**, 294–307.
24. Rawlence, C. and Crichton-Miller, E. (1996) The island of the colour blind. In Rawlence, C. and Crichton-Miller, E. (prods), *The Mind Traveller*. Television documentary series, Rosetta Pictures, London, UK.
25. Miller, S.A., Dykes, D.D. and Polesky, H.F. (1988). A simple salting out procedure for extracting DNA from human nucleated cells. *Nucleic Acids Res.*, **16**, 1215.
26. Wissinger, B., Jägle, H., Kohl, S., Broghammer, M., Baumann, B., Hanna, D.B., Hedels, C., Apfelstedt-Sylla, E., Randazzo, G., Jacobson, S.G. *et al*. (1998). Human rod monochromacy: linkage analysis and mapping of a cone photoreceptor expressed candidate gene on chromosome 2q11. *Genomics*, **51**, 325–331.
27. Ott, J. (1991) *Analysis of Human Genetic Linkage*. Johns Hopkins University Press, Baltimore, MD.
28. Green, E.D., Hieter, P. and Spencer, F.A. (1999) Yeast artificial chromosomes. In Birren, B., Green, E.D., Klapholz, S., Myers, R.M., Riethman, H. and Roskams, J. (eds), *Genome Analysis: A Laboratory Manual*, Vol. 3. Cold Spring Harbor Laboratory Press, Cold Spring Harbor, NY, pp. 297–565.